

10 December 2009

Z. Salman
54 57
WLGA / U119
Zaher.Salman@psi.ch

LEM Group

None

Simulating the LEM beamline transmission and carbon foil scattering using Geant4

Introduction

Geant4 simulations were used to implement the full beamline (at the time of writing, i.e. before the spin rotator). The purpose of these simulations is to test the reliability of current version of Geant4 (4.9.3p2) in predicting muons' scattering from the carbon foil in the trigger detector. Previous versions of Geant4 have been poor in reproducing experimental beam line transmission, mainly due to underestimating scattering from the carbon foil. For example, Paraíso et. al. [1] had to implement the Meyer scattering [2] in order to estimate the transmission of the LEM beam line using Geant4 are reproduce experimental results. However, such implementation into Geant4 was not forward compatible and required heavy programing to implement it into Geant4.

Meanwhile, Geant4 scattering processes implementation have evolved dramatically in the last few years, allowing better tweaking of scattering parameters, which in turn enabled reproducing the expected scattering from the basin (and fast) "Multiple Scattering" physics process. Kamil Sedlak made some initial tests to compare different scattering processes in Geant 4.9.3 through a thin carbon foil. In Fig. 1 I plot the number of scattered muons from a thin carbon foil as a function of angle, limited to small angles. One can see that the scattering as a function of angle is very similar for all processes implemented in Geant4, but it is also similar to that expected from Meyer scattering [3].

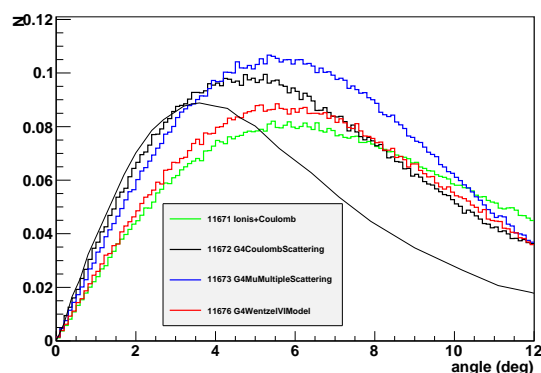


Figure 1: The normalized number of scattered muons as a function of scattering angle.

Transmission of beamline prior spin rotator

Following these results, I performed a full simulation of the full beamline, using parameters similar

to those used by Sedlak for multiple scattering, to compare with the numerical and experimental of Ref. [1]. In these simulations I used the following parameters ¹:

```
#####
##### P H Y S I C S       P R O C E S S E S #####
#####
# Geant 4.9.3
/musr/command process addDiscreteProcess gamma G4PhotoElectricEffect
/musr/command process addDiscreteProcess gamma G4ComptonScattering
/musr/command process addDiscreteProcess gamma G4GammaConversion
/musr/command process addDiscreteProcess gamma G4RayleighScattering
/musr/command process addProcess          e-   G4eMultipleScattering    -1  1  1
/musr/command process addProcess          e-   G4eIonisation           -1  2  2
/musr/command process addProcess          e-   G4eBremsstrahlung       -1  3  3
/musr/command process addProcess          e+   G4eMultipleScattering    -1  1  1
/musr/command process addProcess          e+   G4eIonisation           -1  2  2
/musr/command process addProcess          e+   G4eBremsstrahlung       -1  3  3
/musr/command process addProcess          e+   G4eplusAnnihilation     0 -1  4
/musr/command process addProcess          mu-  G4MuMultipleScattering  -1  1  1
/musr/command process addProcess          mu-  G4MuIonisation          -1  2  2
/musr/command process addProcess          mu-  G4MuBremsstrahlung     -1  3  3
/musr/command process addProcess          mu-  G4MuPairProduction      -1  4  4
/musr/command process addProcess          mu+  G4MuMultipleScattering  -1  1  1
```

The full beam center, envelope and transmission properties are shown in Fig. 2 for different muon initial energies. Note that the largest transmission loss occurs in the trigger detector (TD), as expected. I also observe a shift in the x direction in the beam position after the TD. This shift is may be due to the electric fields in the trigger detector between the different grids, which are not perpendicular to the beam axis. From these simulations we extracted the transmission from the TD to the sample. These values are plotted in Fig. 3 as a function of energy and compared to the results presented in Ref. [1]. The results of the current simulations are in very good agreement with the experimental values. Therefore, we conclude that Geant4.9.3p2 can reproduce realistic scattering in the thin carbon foil used in the trigger detector.

¹An example macro file can be found with this document

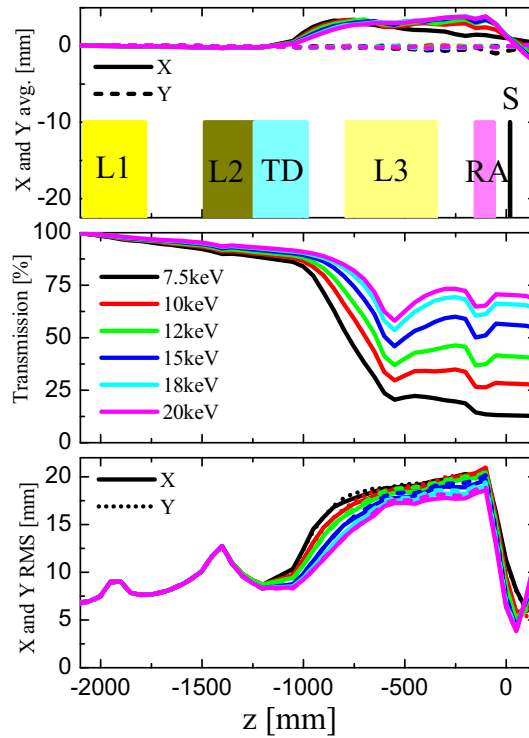


Figure 2: The average position of the muon beam (top), its transmission and root mean square (bottom) as a function of z (along beam axis). The different colors indicate different transport settings at the moderator (beam energy). The solid and dashed lines in the top and bottom panels indicate values in the x and y directions, respectively.

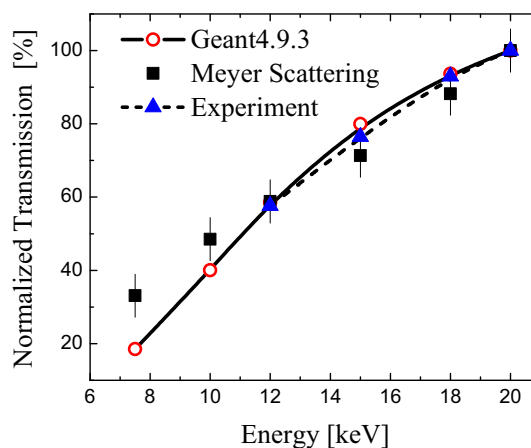


Figure 3: The transmission from before the trigger detector until the sample as a function of beam energy. The circles are values estimated from the current simulations with Geant4.9.3p2, the squares are estimates using the Geant4 with Meyer scattering [1], and the triangles are experimental values. All values were normalized to those on 20keV beam energy.

Transmission of beamline with spin rotator

Turning now to the new beamline with the spin rotator (SR). Below I present results of simulations of the new beamline to evaluate its performance, and compare that with the current situation. We distinguish between two cases, (I) with the spin rotator turned off, i.e. separator mode or TF mode and (II) with the spin rotator on, i.e. rotator (90 degrees) mode or LF mode.

I followed a lengthy tuning procedure for the beam line for various initial beam energies.

1. Initially, working in the separator mode (SR off), I tune the settings of L1 and L3 to obtain maximum transmission trough the beamline up to the carbon foil in the trigger detector (TD).
2. Next, I use the optimal settings of L1 and L3 to tune the electric and magnetic fields of the SR. The aim here is to obtain a 90° spin rotation. For this tuning procedure I use a point like parallel muon beam.
3. Finally, using the tuned SR, I optimise the settings of L1 and L3 again to obtain maximum transmission through the beamline until the carbon foil.

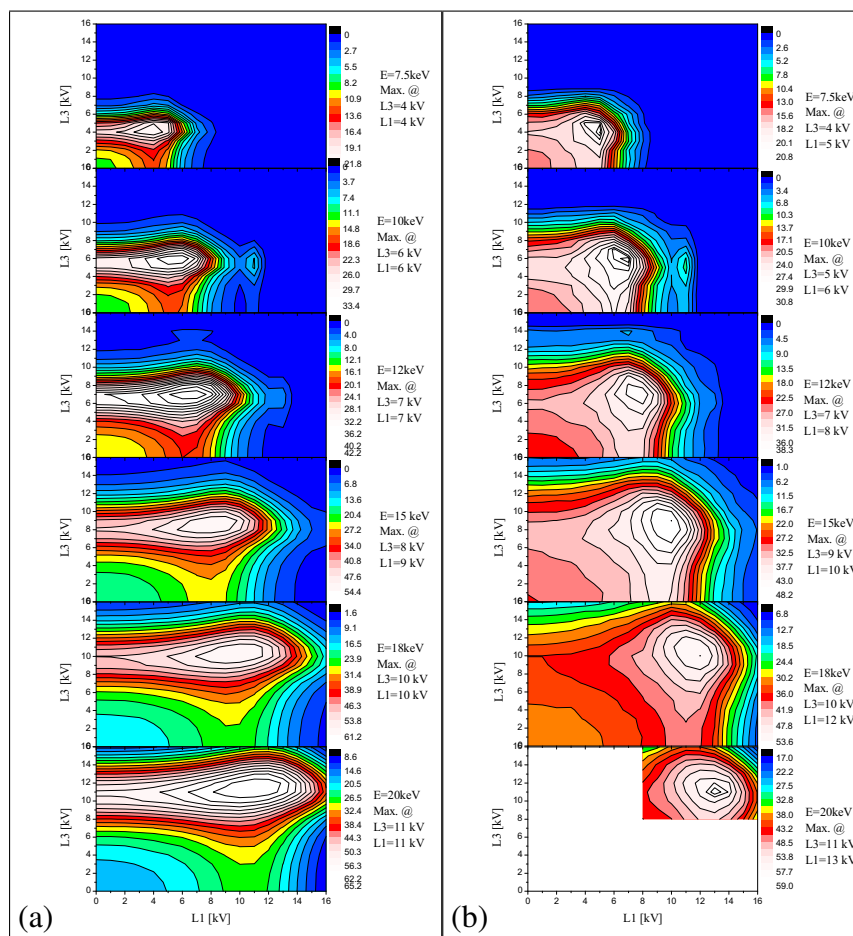


Figure 4: The transmission as a function of L1 (x-axis) and L3 (y-axis). The color coding represents the transmission value in percent. (a) SR off, separator mode and (b) SR on, rotator mode.

Tuning the beamline in separation mode

For this purpose, I set up a template macro file for the simulation, where we loop over settings of L1 and L3, both from 0 kV up to 16kV. For each L1 and L3 setting (with fixed TD and RA), I calculate the beam properties along the beam line and eventually the transmission until the carbon foil. These simulations were repeated for different initial beam energy. The results are summarised in Fig. 4, where we plot a contour plot of the transmission as a function of L1 and L3 settings. From this plot we obtain the best settings of L1 and L3, shown in Table 1.

Beam Energy (keV)	RA (kV)	L1 (kV)	L3 (kV)
20	14.5	11	11
18	12.9	10	10
15	11.0	9	8
12	8.25	7	7
10	6.7	6	6
7.5	4.75	4	4

Table 1: The optimal values of L1 and L3 settings for different beam energies.

The beam properties along the beam line are summarised in Fig. 5.

Tuning the SR with point-like parallel beam

Subsequently, the optimised L1 and L3 settings were used to tune the spin rotator to obtain 90° rotation. In this procedure we use a macro file with fixed L1, L3, RA, and TD settings, appropriate for the beam energy used. Then we change the electric and magnetic field of the SR to obtain a 90° rotation of the spin, maintaining and centered beam at the carbon foil. Note that this procedure should not depend on the settings of L1 and L3 since the beam is an ideal beam, i.e. entering at the center of the SR and parallel to its axis. The results of these simulations are summarised in Table 2. In this table the electric field is given in units of kV, and indicates the potential difference required

Beam Energy (keV)	E field (kV)	B field (Tesla)
20	16.82	-0.0380
18	15.43	-0.0367
15	12.855	-0.0335
12	10.300	-0.0300
10	8.385	-0.0268
7.5	6.315	-0.0233

Table 2: The tuned values of the electric and magnetic field in the spin rotator for a 90° rotation for different beam energies.

on the 37cm long electrode plates.

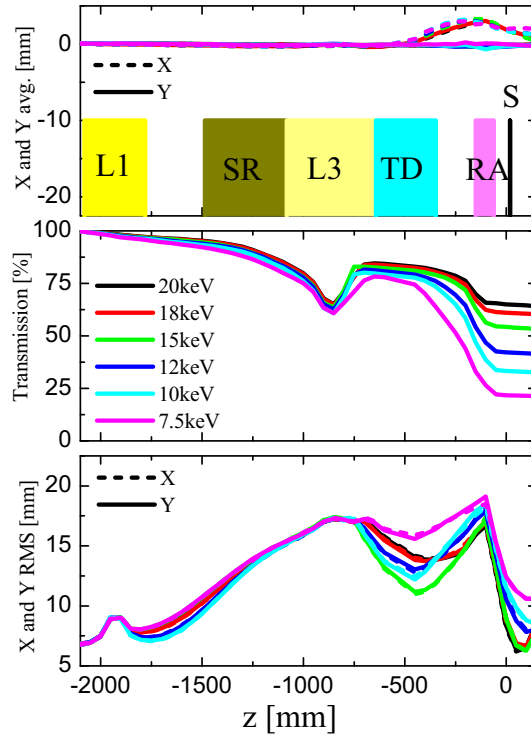


Figure 5: The average position of the muon beam (top), its transmission and root mean square (bottom) as a function of z (along beam axis). The different colors indicate different transport settings at the moderator (beam energy). The solid and dashed lines in the top and bottom panels indicate values in the x and y directions, respectively.

Optimizing L1 and L3 with SR on

Using the previous tunes for 90° rotation in the SR, I optimised the settings of L1 and L3. This is achieved as was done in the separator mode, i.e. by looping over the settings of L1 and L3 from 0 up to 16 kV. The results of these simulations are shown in Fig. 4(b). From these we can extract the optimised values shown in Table 3. Note that the results of this optimization show that in comparison with the settings in separator mode, L3 is almost unchanged, while the voltage of L1 has to be increased by 1-2 kV for the same beam energy.

The beam properties for the optimal settings of L1 and L3 along the beam line are summarised in Fig. 6. Finally, in Fig. 7 we present the transmission as a function of beam energy for different SR operation modes in comparison to the transmission in the current beamline.

Beam Energy (keV)	RA (kV)	L1 (kV)	L3 (kV)
20	14.5	13	11
18	12.9	12	10
15	11.0	10	9
12	8.25	8	7
10	6.7	7	6
7.5	4.75	5	4

Table 3: The optimal values of L1 and L3 settings for different beam energies with the spin rotator set for 90° rotation.

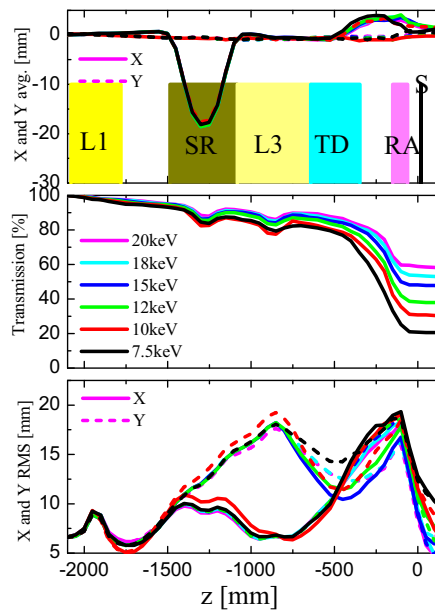


Figure 6: The average position of the muon beam (top), its transmission and root mean square (bottom) as a function of z (along beam axis). The different colors indicate different transport settings at the moderator (beam energy). The solid and dashed lines in the top and bottom panels indicate values in the x and y directions, respectively.

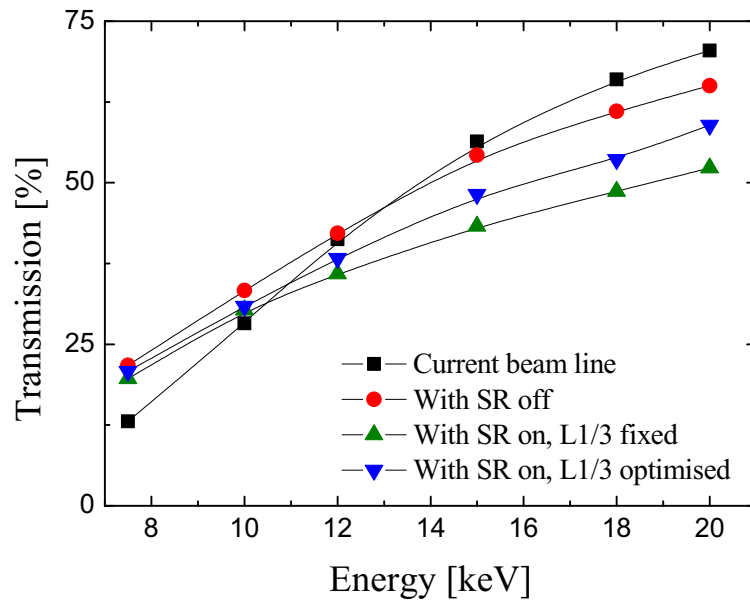


Figure 7: The transmission as a function of energy for the current beamline compared to the different spin rotator operation modes.

- [1] T. Paraiso, E. Morenzoni, T. Prokscha, and A. Suter, *Physica B* **374-375**, 498 (2006).
- [2] L. Meyer, *Phys. Stat. Solidi (b)* **44**, 253 (1971).
- [3] A. Hofer, PhD. Thesis (1998).